Lipid levels in sperm, eggs, and during fertilization in *Xenopus laevis*

Douglas W. Petcoff,[†] William L. Holland,[*] and Bradley J. Stith[1,*]

Department of Biology,[*] University of Colorado Denver, Denver, CO; and Metropolitan State College,[†] Denver, CO

Abstract **Critical developmental periods, such as fertilization, involve metabolic activation, membrane fusion events such as sperm-egg or plasma membrane-cortical granule merger, and production and hydrolysis of phospholipids. However, there has been no large-scale quantification of phospholipid changes during fertilization. Using an enzymatic assay, traditional FA analysis by TLC and gas chromatography, along with a new method of phospholipid measurement involving HPLC separation and evaporative light-scattering detection, we report lipid levels in eggs, sperm, and during fertilization in *Xenopus laevis*. Sperm were found to contain different amounts of phospholipids as compared with eggs. During fertilization, total phosphatidylinositol, lysophosphatidylcholine, sphingomyelin, and phosphatidylserine decreased, and ceramide increased, whereas there was no change in phosphatidylcholine, cardiolipin, or phosphatidylethanolamine. FA analysis of phospholipids found numerous changes during fertilization. Because there is an increase in *sn*-1,2-diacylglycerol at fertilization, the FAs associated with this increase and the source of the increase in this neutral lipid were examined. Finally, activation of phospholipase C, phospholipase D, phospholipase A2, autotoxin, and sphingomyelinase at fertilization is discussed.—**Petcoff, D. W., W. L. Holland, and B. J. Stith. **Lipid levels in sperm, eggs, and during fertilization in *Xenopus laevis*. *J. Lipid Res.* 2008.** 49: **2365–2378.**

Supplementary key words diacylglycerol • phospholipase C • phospholipase D • phospholipase A2 • autotaxin • sphingomyelinase

Major goals of the LIPID Metabolites and Pathways Strategy (LIPID MAPS) are to "separate and detect all of the lipids in a specific cell," "to quantitate each of the lipid metabolites present and determine the changes in their levels," and to study lipid metabolic pathways during biological events (1). Characterizing changes in the lipid composition during defined biological events is part of the concept of "functional lipidomics" (2). These fundamental, descriptive studies will facilitate our understanding of how lipids regulate membrane fluidity and fusion, lipid rafts, the cytoskeleton, kinases, and protein binding to membranes (e.g., 3–5) to induce pleiotropic cellular effects.

About 15 years ago, quantification of lipid mass changes during maturation of the oocyte to the fertilizable egg, and during fertilization of the egg by sperm, was begun in *Xenopus laevis* (6–9). Critical developmental events can be isolated in vitro with this model system, and large numbers of gametes can be obtained to provide sufficient amounts of second messengers and lipids. During fertilization, membrane bending and fusion are associated with the acrosome reaction of sperm (wherein the large sperm acrosome undergoes exocytosis upon interaction with layers that cover the egg), with sperm-egg merger, and with subsequent fertilization events such as cortical granule exocytosis (10, 11). Furthermore, both *Xenopus* and human eggs are arrested in meiosis II (12).

Compared with oocytes, one disadvantage of studying eggs is that they have a short life, much less than the estimated time for lipid precursor incorporation to near equilibrium levels (6, 7). Thus, lipid analysis based on label incorporation or turnover is not reliable, and methods that directly measure lipid mass are needed for fertilization studies.

LIPID SIGNALING RELATED TO FERTILIZATION

In terms of lipids in sperm, capacitation (13), alcoholism (14), storage (15), and passage through the epididymis (16) or cervical mucus (17) have been found to alter lipid composition. Although there are many studies on lipids in sperm, there has been no comprehensive, comparative study on the lipid composition of eggs versus sperm, or

This work has been supported by National Science Foundation Grant IBN-0110609, and University of Colorado Denver Downtown Campus Undergraduate Research Opportunity Program grants.

Manuscript received 27 March 2008 and in revised form 23 June 2008.

Published, JLR Papers in Press, June 24, 2008.
DOI 10.1194/jlr.M800159-JLR200

Abbreviations: CL, cardiolipin; DAG, diacylglycerol; DHA, docosahexaenoic acid; ELSD, evaporative light-scattering detection; EPA, eicosapentaenoic acid; IP3, inositol 1,4,5-trisphosphate; LPC, lysophosphatidylcholine; MBS, modified Barth's medium; MUFA, monounsaturated fatty acid; PA, phosphatidic acid; PC, phosphatidylcholine; PE, phosphatidylethanolamine; PI, phosphatidylinositol; PIP2, phosphatidylinositol 4,5-bisphosphate; PKC, protein kinase C; PLD, phospholipase D; PS, phosphatidylserine; SM, sphingomyelin.

[1] To whom correspondence should be addressed.
e-mail: brad.stith@cudenver.edu

their changes during fertilization. Thus, the following lipids have been examined during fertilization in *Xenopus laevis*.

Lysophosphatidylcholine (LPC) has been suggested to induce membrane fusion, and it can induce the acrosome reaction of sperm (18). LPC can stimulate tyrosine kinases (18), phospholipase C (PLC), and map kinases (19). Phospholipase A2 (PLA2) breaks down phosphatidylcholine (PC) to LPC, and it is interesting to note that a PLA2 inhibitor inhibited fertilization envelope formation during sea urchin fertilization but did not block the increase in $[Ca++]_{in}$ or acid efflux/zygote alkalinization (20). Furthermore, Riffo and Parraga (21) suggest that PLA2 activation is important in sperm-egg fusion, inasmuch as LPC addition induced the interspecies fusion of human sperm and the hamster egg and anti-PLA2 antibodies were inhibitory.

Plasmalogens, in which instead of an ester bond, a vinyl ether bond is located at the *sn*-1 position of the glycerol backbone, have been suggested to protect sperm from oxidation and to play a role in sperm-egg fusion (22, 23).

Cardiolipin (CL) is found predominantly (80%) in mitochondria, whereas about 16% is in the nuclear envelope and 4% in the plasma membrane (24). CL binds calcium with higher affinity than PC, phosphatidylethanolamine (PE), or phosphatidylserine (PS) (24), and this binding is associated with stabilization of the hexagonal phase of the membrane and destabilization of the lamellar phase. Thus, CL may alter membrane properties to facilitate membrane bending and fusion during sperm union with the egg (25). In fact, CL has been found to enhance sperm-vesicle fusion (26), antibodies to sperm surface CL may decrease fertility (27, 28), and the lipid may be concentrated at the surface of sperm in the region of fusion (29).

The presence of certain lipids affects the stability of membrane rafts (detergent-insensitive density membrane fractions with high levels of saturated phospholipids) (30). For example, sphingomyelin (SM) stabilizes rafts and may play a role in membrane fusion (31). Membrane rafts have been described in *Xenopus laevis* eggs (32), and it is believed that sperm-egg interaction occurs through these rafts (33–35).

Sperm membranes obtain large amounts of phospholipids with polyunsaturated fatty acids (PUFAs) as they move through the epididymis (16). This decrease in lipid saturation has been suggested to increase membrane fluidity, affect rafts, and provide protection against oxidation (36). One PUFA, 22:6n3 (docosahexaenoic acid or DHA), is prevalent in sperm (16, 36) and has been found to decrease the amount of diacylglycerol (DAG) in rafts, possibly induce raft SM degradation to ceramide, and increase apoptosis in cancer cells (30).

Inasmuch as C_2-ceramide or an inhibitor of alkaline ceramidase can enhance calcium ionophore induction of the acrosome reaction in boar sperm, ceramide may be involved in the acrosome reaction of sperm (37). Ceramide can be produced by degradation of SM, and SM inhibits whereas ceramide facilitates sperm capacitation (38).

The short half-life of eggs (39) is due to ceramide that induces apoptosis (40, 41). Ceramide may also form membrane channels for proteins like cytochrome C, and stabilize membrane rafts (42). The early embryo is resistant to apoptosis, owing to low levels of ceramide (43, 44); however, there has been no measurement of ceramide during fertilization.

Activation of PLC has been noted as the central pathway in fertilization. Activation of this enzyme and production of inositol 1,4,5-trisphosphate (IP3) and *sn*-1,2 diacylglycerol (DAG) from phosphatidylinositol 4,5-bisphosphate (PIP2) may be sufficient to induce all events of fertilization [for *Xenopus*: (7, 8, 45, 46)]. Much work by Sato and associates (46) suggests that *Xenopus* sperm activate Src tyrosine kinase, which, in turn, activates PLC-γ.

Our prior work showed that *sn*-1,2-DAG mass increased 48 pmol per cell (from 62 to 110 pmol/cell) and peaked at about 10–15 min after insemination (9). A translocation of DAG-dependent protein kinase C (PKC) α and β to a membrane fraction was also noted. PKC may be involved in resumption of endocytosis (47, 48), cortical contraction, cortical granule exocytosis, chromosome decondensation, nuclear envelope and Golgi reformation, and cleavage furrow formation in *Xenopus laevis* (49, 50).

DAG may act independently of PKC; for example, it may play a role in sperm-egg fusion in the sea urchin, because neomycin (which presumably inhibits DAG production by binding to PIP2) inhibits sperm-egg fusion but calcium chelators do not (51). One DAG species, 18:0/20:4 DAG, induces fusion of vesicles to form a nuclear envelope around sperm DNA in the egg cytoplasm (a fertilization event) (52).

By comparing the time course and size of the increase in DAG mass to the increase in IP3 mass at fertilization [the IP3 increase is about 280 times lower and peaks ~5–10 min before that of DAG; (7, 8)], and considering that precursor PIP2 mass is never greater than 2 pmol per *Xenopus* zygote (45), production of 48 pmol of DAG from PIP2 would be unlikely (9). Because choline mass increases on a magnitude equivalent to the increase in DAG, we suggested that breakdown of PC by phospholipase D (PLD) is the source of DAG (9). PLD would hydrolyze PC to phosphatidic acid (PA), which would be dephosphorylated to DAG (53). There was no detectable change in phosphocholine, and there is no known eukaryotic PC-specific PLC that would produce DAG and phosphocholine from PC. To search for the source of the DAG increase at fertilization, we compare decreases in individual FAs in phospholipids with increases in those in DAG.

In summary, we report the mass of major phospholipid classes and their FAs: CL, PE, PS, phosphatidylinositol (PI), PC, LPC, and SM in *Xenopus laevis* sperm, eggs, and through fertilization. Lipids are analyzed by three methods: an enzymatic assay of ceramide by DAG kinase, a traditional approach involving TLC followed by gas chromatography, and a new method involving HPLC separation and evaporative light-scattering detection (ELSD) (54).

MATERIALS AND METHODS

Xenopus gametes and fertilization

Fertilization protocols have been published (7–9), but are briefly described here. To obtain eggs, *Xenopus* females were

primed 3–10 days before use with 100 IU of pregnant mare's serum gonadotrophin (Calbiochem-EMD Biosciences) in 0.1 mg/ml BSA (Sigma Chemical Co.). Then, 8–12 h before use, primed females were injected with 850 IU of human chorionic gonadotrophin (Sigma Chemical Co.) to induce ovulation. Eggs were kept in 100% modified Barth's medium (MBS) (pH 7.5; 88 mM NaCl, 1 mM KCl, 2.4 mM $NaHCO_3$, 10 mM *N*-2-hydroxyethylpiperazine-*N*′-2-ethanesulfonic acid, 0.82 mM $MgSO_4 \cdot 7H_2O$, 0.33 mM $Ca(NO_3)_2 \cdot 4H_2O$, 0.41 mM $CaCl_2 \cdot 2H_2O$). Just before fertilization, eggs were rinsed twice with and then placed into 1 ml of 10% MBS. To obtain a suspension of sperm, two testes from a *Xenopus laevis* male were minced in 2.4 ml of 100% MBS. For fertilization, 167 μl of the minced testes solution (~9.47 million sperm) was added to the eggs. The rate and success of insemination were recorded by evaluation of video tapes that record the percentage of cells that undergo gravitational rotation (the dark animal pole rotates upward by 15 min after insemination) and cleavage (at about 100 min), typically a 100% success rate.

Extraction of lipids from *Xenopus* cells

Depending upon the phospholipid to be measured, different numbers of eggs or zygotes were extracted: for PE and PC, groups consisting of 3 eggs were used. For PI and SM, 15 eggs per group were used, and for PS, PI, and SM, 80 eggs were used. For analysis of sperm, 1 ml of testes solution (~56.7 million sperm) was extracted.

Because our method of lipid extraction for major phospholipid classes has been described (54), we briefly note that 40 s before the desired time point, excess MBS was removed and the eggs or zygotes were washed with 10% MBS (there was no washing for the 1 ml sperm suspension). For the zygote samples, we chose 5 min after insemination because we have found that PLC activation and DAG increased at this time (8, 9). Then, 1 ml of 1:2 chloroform-methanol was added and cells were homogenized with 20 strokes in a Dounce homogenizer (prefilled with N_2). The mortar and pestle were then washed with 0.5 ml chloroform. This was followed by two washes with 0.5 ml of 1 M NaCl (our experience suggests that high salt drives anionic lipids into the organic phase, whereas acidic methanol-chloroform can degrade lipids). The extracts were centrifuged (clinical centrifuge; 500 *g*, 2 min), and the organic layer was transferred to a fresh, chilled test tube and kept under N_2.

HPLC separation and ELSD of major phospholipid classes

After drying under N_2 (N-Evap; Organomation Associates, Berlin MA), the sample was resolubilized in 80:19:1 chloroform-methanol-water and injected into a normal-phase silica column on a dual pump HPLC (Rainen HPXL) (54). A ternary gradient of chloroform with increasing amounts of methanol and water was used to elute lipids (54). A Sedex 55 evaporative light scattering detector (Richard Scientific) was used to record the mass of phospholipids. At our settings (54), the detector has a practical lower limit of about 1 nmol (or 1 μg; using an average phospholipid of 780 Da and a minimal peak size of about 50,000 μV-sec). We used the mass of standards (Avanti Polar Lipids, Inc., Alabaster AL), the ELSD response, and an average molecular mass for each phospholipid to calculate the amount of the *Xenopus* phospholipid in nanomoles. Average molecular mass was: for PC, 760 Da; for PE, 757 Da; for PI, 909 Da; for SM, 745 Da; and for PS, 810 Da.

FA analysis of lipids

For analysis of FAs connected to the various lipids, *Xenopus* eggs or zygotes (5 min after insemination) were extracted for lipids (see above) and lipid classes were separated by TLC (55). Individual lipids were then transesterified (3 N methanolic-HCl, sealed vials, under nitrogen, at 100°C for 45 min), and the resulting FA methyl esters were extracted (hexane, 0.05% butylated hydroxytoluene), separated, and quantified by capillary gas chromatography (Hewlett-Packard model 6890, Wilmington, DE), using a 30 m DB-225MS capillary column (J and W Scientific, Folsom, CA) and a flame-ionization detector (55). Comparisons with known FA standards identified peaks, and standards for recovery efficiency were included. The data for the mole percent of each FA represent the amount of a FA multiplied by 100 and divided by the total FA in that particular lipid class. Data for the mole percent of a class of phospholipid are the total amount in the lipid class multiplied by 100 and divided by the total of all major phospholipid classes.

For sperm DAG FA analysis, two testes were minced in 2.4 ml of 100% MBS, and 0.5 ml of this sperm suspension was extracted for lipids with 2:1 chloroform-methanol (followed by phase separation and chloroform isolation as noted above). This amount of sperm should produce amounts of lipid similar to the egg sample. For eggs, 10 cells were placed in 1 ml of 100% MBS and extracted as with sperm. Zygotes were obtained at 12 min after insemination (when maximal levels of DAG are achieved) (9), and lipids were extracted as noted above. For zygotes, fertilization was achieved by addition of 50 μl of sperm suspension in 100% MBS to groups of 10 eggs in 300 μl of 20% MBS. Before extraction, excess sperm were washed away. FA species of DAG were determined by gas chromatography as noted above.

Ceramide mass measurement

The amount of ceramide was determined by use of a DAG kinase assay developed by Bell and associates [(56); for a detailed procedure using *Xenopus* oocytes, eggs, and zygotes, see Refs. 9, 57)]. Lipids were extracted as noted above and were phosphorylated with [^{32}P]ATP (ICN, Costa Mesa, CA) and DAG kinase (EMD/Calbiochem, Inc., La Jolla, CA). The labeled ceramide phosphate was purified by TLC, and the radioactivity was quantified by liquid scintillation counting. Standards (Avanti Polar Lipids) were used to calculate the amount of ceramide per cell.

Statistics

Data were analyzed by two-sided Student's *t*-test, which was calculated by Sigmaplot 2001 (version 7.101). The average ± the standard error, along with the sample size (e.g., n = 3), are stated in the text and shown in the figures.

RESULTS

Lipids in *Xenopus* sperm and eggs

Using our new method of phospholipid analysis by HPLC and ELSD, sperm were found to contain a very different ratio of phospholipids than that found in eggs (**Fig. 1**). Approximately equal volumes of cells were used for comparison. In a second comparison, data from sperm and eggs were transformed into mole percent and compared directly (**Fig. 2**).

Sperm have ~40% higher levels of PE than eggs, but sperm have much less PC (only 25% of the PC found in eggs). There were ~7-fold higher amounts of PS and ~3-fold greater amounts of SM in sperm than in eggs. There was no obvious difference in the relative amounts of PI in eggs or sperm.

Because DAG is an important second messenger, the total amount of DAG (all diesters of glycerol, e.g., en-

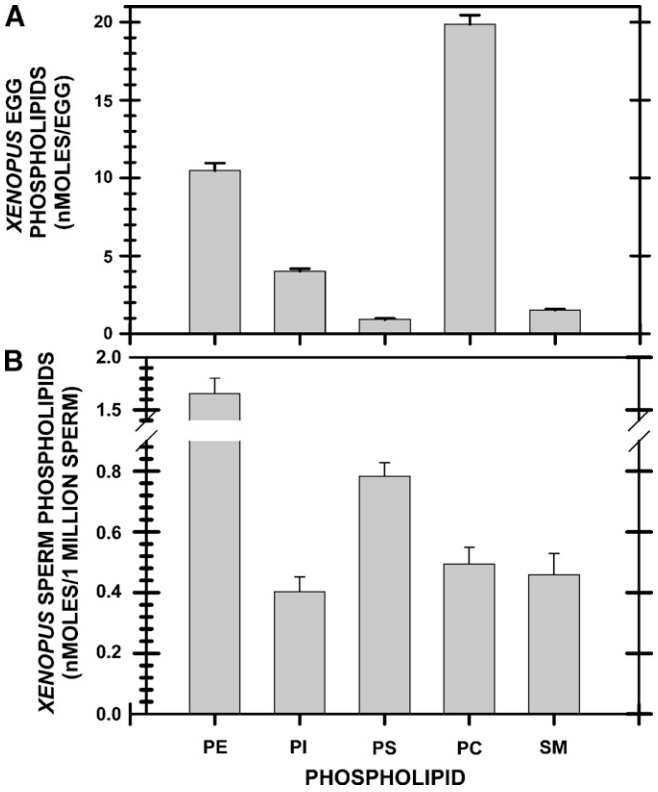

Fig. 1. *Xenopus* sperm and egg phospholipids. Cells were extracted, separated by HPLC, and mass amounts were recorded by evaporative light-scattering detection (ELSD) and use of a standard line for each lipid. The values for 1 million sperm (B), the approximate volume of one *Xenopus* egg, were used to facilitate comparison with the eggs (A). PE, phosphatidylethanolamine; PI, phosphatidylinositol; PS, phosphatidylserine; PC, phosphatidylcholine; SM, sphingomyelin. Error bars indicate SEM.

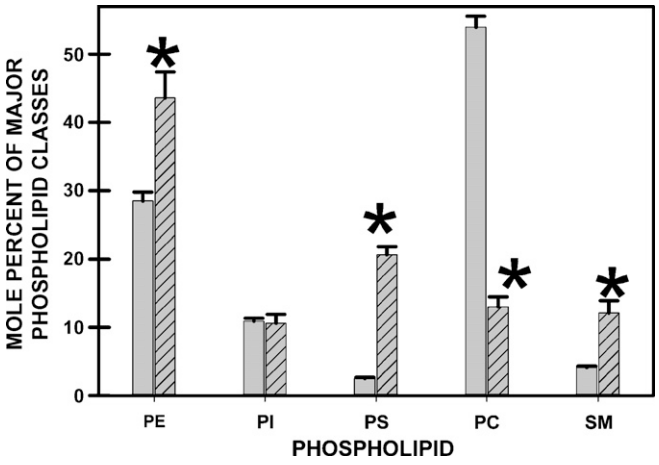

Fig. 2. A comparison of *Xenopus* egg and sperm phospholipids. Based on HPLC/ELSD methodology, the mole percent of the major classes of phospholipids from *Xenopus* eggs (open bar) and from sperm (hatched bar) were compared. The amount of each phospholipid was multiplied by 100 and divided by the total mass of all major lipids. When sperm were compared with eggs, significant differences were noted with an asterisk ($P < 0.05$).

antiomeric *sn*-1,2/2,3 and isomeric *sn*-1,3) determined by TLC/gas chromatography was 531 pmol in *Xenopus* eggs, 571 pmol in zygotes (12 min after insemination), and 1,238 pmol in sperm (a sperm sample estimated to be the same volume as one *Xenopus* egg) (**Fig. 3A**). This increase in total DAG (40 pmol) is similar to that we reported earlier for *sn*-1,2 DAG (48 pmol), which was measured by the DAG kinase assay (9). If basal levels of the *sn*-1,2 form of DAG are about 62 pmol (9), and total DAG is 531 pmol, then the *sn*-1,2 form of DAG makes up only ~12% of all DAG forms.

The different FAs of DAG in both sperm and eggs were compared (Fig. 3). **Table 1** has a guide to the 40 FAs shown in the figures. As compared with eggs, sperm contain more 16:0 (peak 5), t16:1n7 (peak 6), 18:0 (peak 11), and 20:4n6 (peak 27). Those FAs of DAG that differ in eggs and sperm are presented in **Table 2**.

There also appears to be more plasmalogen dm18:1n9 in DAG (peak 9; which is not detectable in egg; Fig. 3) in sperm.

Changes in major phospholipid classes through fertilization

After fertilization, PI decreased by 1.17 nmol per cell (**Fig. 4**; **Table 3**), whereas total PE and PC did not change at fertilization. The level of PS dropped 234 pmol at 3 min (0.916 ± 0.057 nmol/egg to 0.682 ± 0.037 nmol/cell, n = 5, $P < 0.01$) but returned to basal levels by 5 min.

The measurement of individual FAs of phospholipids by gas chromatography showed that there was a significant decrease in 18:1n9 PC (peak 13) from 12.665 ± 0.0531 mol% in the egg to 12.355 ± 0.074 mol% in the zygote (n = 3 each; $P < 0.027$) (top panel, **Fig. 5**).

In analysis of a combined PI/PS fraction during *Xenopus* fertilization, the largest change was a drop in 18:1n9 (11.383 ± 0.270 mol% to 6.691 ± 0.265 mol%; n = 3 each, $P < 0.00024$), and there were additional decreases in 16:0 (peak 5), 16:1n7 (peak 7), and 18:0 (peak 11) (Fig. 5). There was an increase in 20:5n3 [eicosapentaenoic acid (EPA), peak 30].

The largely mitochondrial lipid CL made up only 0.75 mol% of all major phospholipids in the *Xenopus* egg. There was no significant change in total CL during fertilization (Table 3), but there was a significant decrease in 16:1n7 CL (from 8.287 ± 0.296 mol% to 6.286 ± 0.599 mol%; n = 3 each, $P < 0.04$) and *trans*-18:1n9 increased (from 0.987 ± 0.391 mol% to 2.247 ± 0.054 mol%; $P < 0.03$), whereas 20:0 doubled (0.483 ± 0.122 mol% to 0.948 ± 0.123 mol%; n = 3 each, $P < 0.05$) (Fig. 5).

These FAs in PE changed during fertilization: 18:1n9 decreased (8.410 ± 0.0183 mol% to 6.629 ± 0.047 mol%; n = 3 each, $P < 0.000003$), and both arachidonate 20:4n6 (14.596 ± 0.272 mol% to 15.311 ± 0.079 mol%; n = 3 each, $P < 0.06$), and 20:5n3 EPA increased (9.402 ± 0.241 mol% to 10.493 ± 0.270 mol%; n = 3 each, $P < 0.04$) (Fig. 5).

The total amount of LPC made up 1.78 mol% of all major phospholipids. During fertilization, LPC mass declined from 1.671 ± 0.234 to 0.869 ± 0.146 nmol per cell (n = 3 each, $P < 0.043$) (Table 3). As shown in Fig. 5, the 18:1n9 LPC decreased from 20.923 ± 0.660 mol% to 13.988 ± 1.183 mol% (n = 3 each, $P < 0.007$), whereas there was

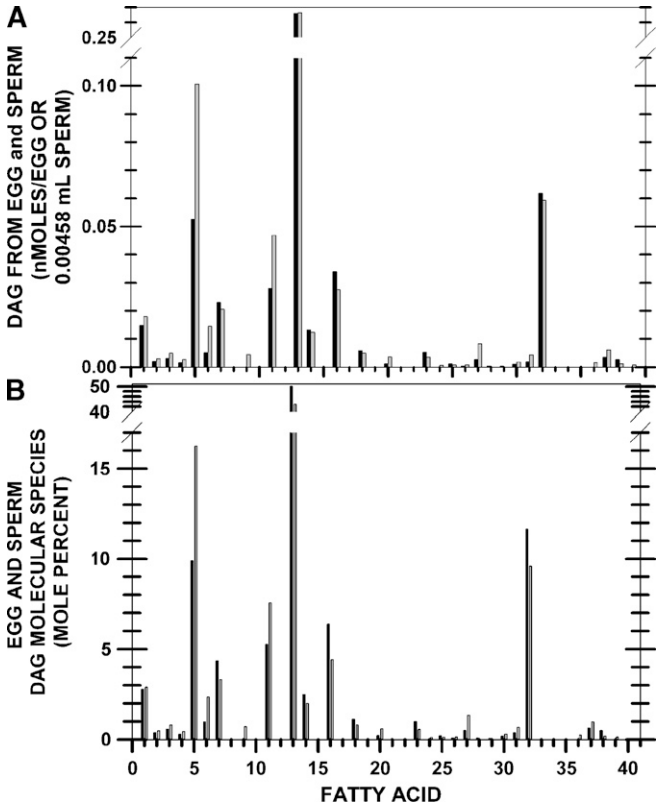

Fig. 3. A comparison of *Xenopus* egg and sperm *sn*-1,2-diacylglycerol FAs. In an analysis by gas chromatography, the different diacylglycerol (DAG) FAs are shown on the abscissa based on the numbering system noted in Table 1. The amount of each DAG FA in egg (first bar) or sperm (second bar of the pair) is shown (A). To be able to compare relative levels of FA in the sperm and egg, the amount of 18:1n9 DAG in sperm was made equivalent to the amount in one egg. Thus, the values for the different molecules of sperm DAG were divided by 109 (this final amount is equivalent to 0.00458 ml). In another method of comparison (B), the mole percents of each DAG FA in either egg or sperm are shown grouped together.

TABLE 1. Numbers on the X axis of Figs. 3, 5, and 8–10 representing different FAs of the phospholipid or DAG and corresponding to the following list

1	14:0
2	14:1n5
3	15:0
4	dm16:0
5	16:0
6	*trans*-16:1n7 (9-*trans*-hexadecenoic acid)
7	16:1n7
8	dm18:0
9	dm18:1n9
10	dm18:1n7
11	18:0
12	*trans*-18:1n9 (9-*trans*-octadecenoic acid)
13	18:1n9
14	18:1n7
15	*trans*-18:2n6
16	18:2n6
17	18:3n6
18	18:3n3
19	18:4n3
20	20:0
21	20:1n15
22	20:1n12
23	20:1n9
24	20:3n9
25	20:2n6
26	20:3n6
27	20:4n6 (arachidonic acid)
28	20:3n3
29	20:4n3
30	20:5n3 (eicosapentaenoic acid, EPA)
31	22:0
32	22:1n9
33	22:2n6
34	22:4n6
35	22:5n6
36	22:5n3
37	22:6n3 (docosahexaenoic acid, DHA)
38	24:0
39	24:1n9
40	24:6n3

DAG, diacylglycerol. Note that n refers to the position of the double bond from the terminal carbon, dm refers to plasmalogens, and *trans* refers to *trans* double bonds.

an increase in 22:6n3 (peak 37; DHA) from 1.998 ± 0.343 mol% to 4.809 ± 0.978 mol% (n = 3 each, $P < 0.05$). The apparent increase in peak 5 (16:0) was not significant (24.75 ± 1.36 mol% to 29.9.975 ± 2.71 mol%; $P < 0.16$; n = 3 each). Similarly, the apparent decrease in peak 6 (t16:1n7) was not significant (11.947 ± 1.12 mol% to 8.93 ± 1.02 mol%, $P < 0.11$; n = 3 each).

Saturation changes through fertilization

Increasing degrees of saturation can lower membrane fluidity and affect other membrane properties. During *Xenopus* fertilization, the mole percent of saturated FAs decreased in PI/PS (43.22 ± 0.73 mol% to 39.42 ± 0.61 mol%; $P < 0.016$; n = 3 each) and increased in SM (50.94 ± 0.60 mol% to 59.45 ± 0.39 mol%; $P < 0.0002$; n = 3 each) (**Fig. 6**).

Monounsaturated fatty acids (MUFAs) decreased in LPC, PC, PE, PI/PS and SM but not in CL (Fig. 6). The largest decreases were in LPC, PI/PS, and SM. MUFA in LPC declined by 29% (26.9 ± 0.5 mol% to 19.1 ± 2.1 mol%; $P < 0.001$; n = 3 each), whereas MUFA in SM decreased 30% (from 35.5 ± 1.4 mol% to 24.9 ± 1.4 mol%; $P < 0.001$; n = 3 each), and in PI/PS declined 35% (17.1 ± 0.6 mol% to 11.2 ± 1.1 mol%; $P < 0.01$; n = 3 each).

PUFA in the PI/PS fraction increased 24% during fertilization (37.2 ± 1.2 mol% to 46.2 ± 1.3 mol%; $P < 0.01$;

TABLE 2. Comparison of DAG data expressed in mole percent

Molecular Species DAG	No. on X Axis	Egg	Zygote	Sperm	Sperm vs. Egg
14:0	1	2.78	2.74	2.88	1.04
16:0	5	9.89	8.95	16.24	1.72
t16:1n7	6	0.98	0.51	2.34	3.14
16:1n7	7	4.34	4.38	3.31	0.78
18:0	11	5.25	4.16	7.57	1.61
18:1n9	13	50.10	52.77	43.03	1.20
18:1n7	14	2.49	2.55	2.00	0.79
18:2n6	16	6.39	6.19	4.44	0.71
22:1n9	32	11.63	12.19	9.60	0.81

The number on the X axis refers to the DAG FA species in Figs. 3, 9, and 10 (see Table 1 for guide). The sperm vs. egg values were obtained by dividing the sperm value for a FA by the egg value.

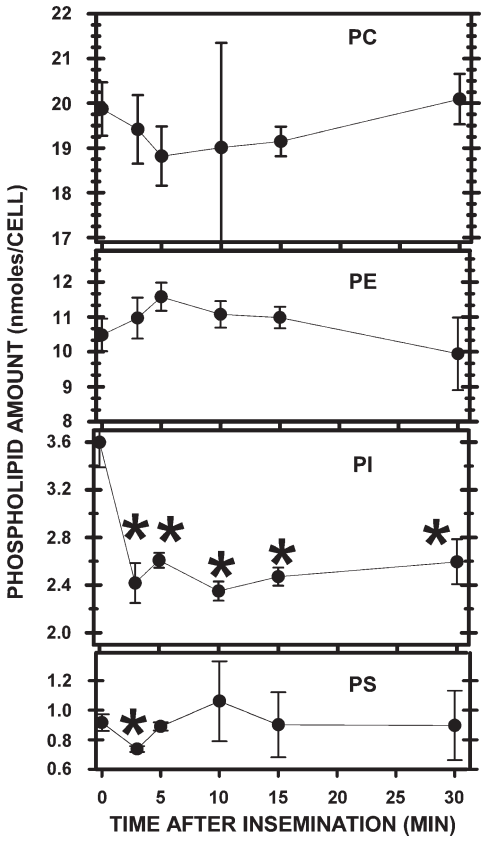

Fig. 4. The mass of major phospholipids during *Xenopus* fertilization. As measured by HPLC/ELSD, samples were obtained after insemination. We previously estimated (7, 9) that sperm-egg contact occurs at ~1 min after insemination. A calcium/surface contraction wave traverses the zygote at ~3–6 min to induce cortical granule exocytosis. Asterisks denote significance at * $P < 0.05$. Error bars indicate SEM.

n = 3 each), whereas that in PE increased, from 46.65 ± 0.49 mol% to 49.08 ± 0.15 mol% ($P < 0.009$; n = 3 each) (Fig. 6). There were no detectable changes in the mole percents of PUFA in CL, LPC, PC, and SM.

TABLE 3. Summary of lipid changes at fertilization

	Egg	Zygote	Change
IP3[a]	0.038	0.211	0.173
DAG[b]	62	110	48
Choline[b]	113	247	134
PC	19,870 ± 590 (7)	19,140 ± 630 (24)	
PE	10,480 ± 470 (20)	11,190 ± 210 (29)	
PI	3,600 ± 209 (22)	2,428 ± 48 (77)	−1,172
PS	916 ± 57 (7)	879 ± 54 (19)	
CL	700 ± 54 (3)	728 ± 23 (3)	
LPC	1,671 ± 234 (3)	869 ± 146 (3)	−802
SM	1,530 ± 60 (28)	1,300 ± 20 (82)	−230
Ceramide	392 ± 30 (9)	600 ± 20 (17)	208

CL, cardiolipin; IP3, inositol 1,4,5-trisphosphate; LPC, lysophosphatidylcholine. Mean ± standard error, pmoles per cell; the number of determinations is in parentheses; a negative sign represents a decrease.

[a] (8).

[b] (9).

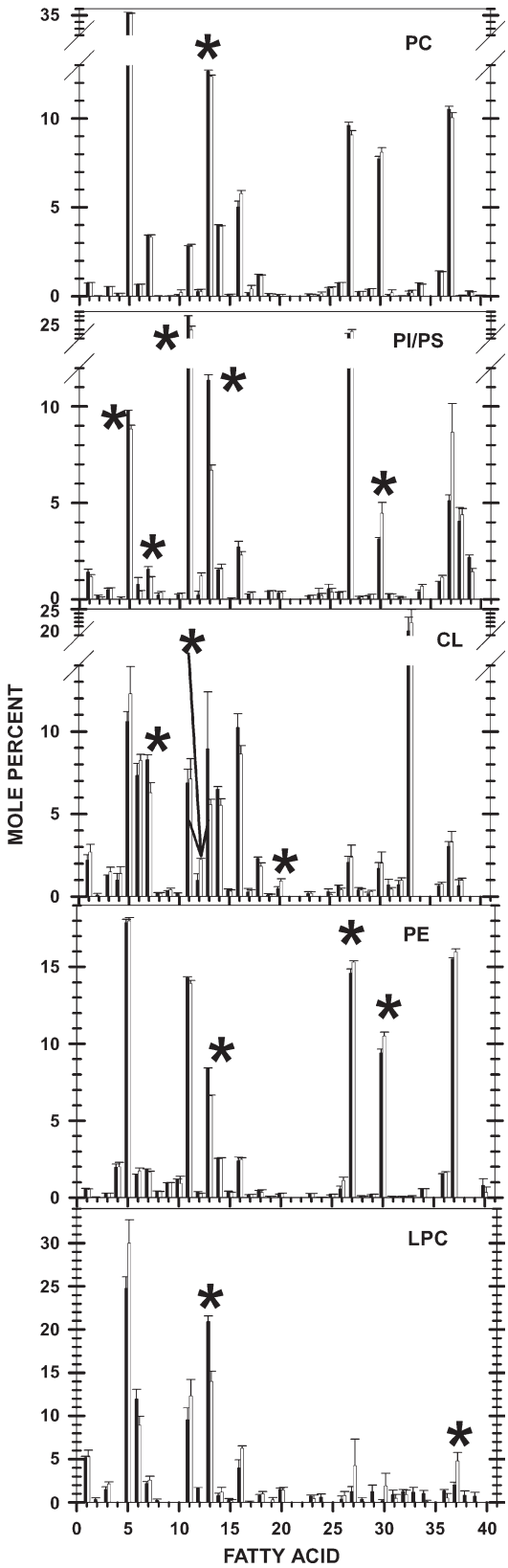

Fig. 5. Changes in FA content of major phospholipids during fertilization. Data are expressed as a mole percent of each lipid class (n = 3 for all determinations). Mole percent was expressed as the percent of each species in each major class of lipid. The different FAs along the abscissa are identified in Table 1. * $P < 0.05$. CL, cardiolipin; LPC, lysophosphatidylcholine. Error bars indicate SEM.

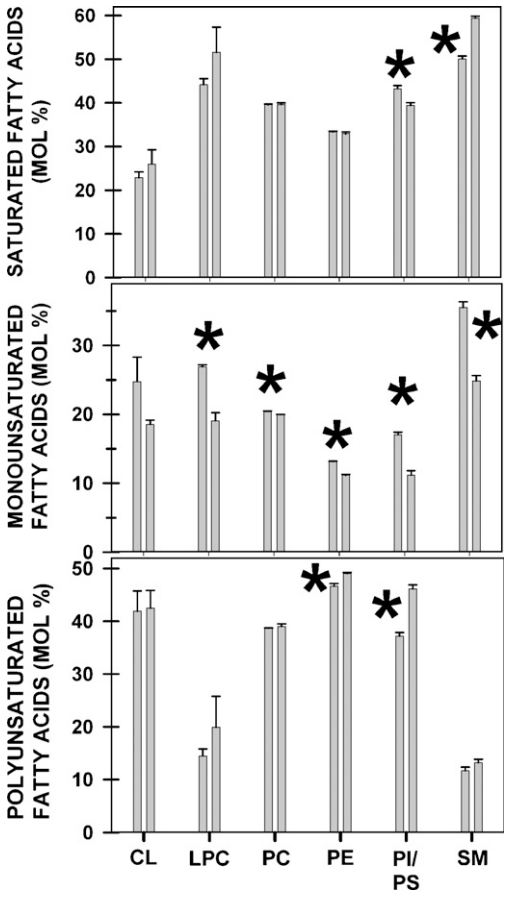

Fig. 6. Saturation changes in fertilization. Within each of the phospholipid classes, the mole percent of saturated (top), monounsaturated (middle), or polyunsaturated (bottom) FAs were determined and graphed. The first vertical bar of each pair represents the egg and the second bar is the zygote. Asterisks denote significance at $P < 0.05$. Error bars indicate SEM.

Plasmalogens in phospholipids

Plasmalogens are detected after acid hydrolysis and subsequent dimethyl (dm) acetyl production. There were no detectable changes in the level of plasmalogens (dm16:0, dm18:0, dm18:1n9, dm18:1n7) during fertilization.

As is typical (23), small amounts of plasmalogens were present in the PC and PE family from the *Xenopus* egg or zygote, and those from other major lipid classes were negligible. The largest plasmalogen PC was dm16:0 PC (0.16 ± 0.003 mol%; n = 6), and dm18:1n7 PC (0.09 ± 0.002 mol%; n = 5), whereas dm18:0 and dm18:1n9 PC were undetectable.

PE plasmalogens were more common than those from PC in the *Xenopus* egg and zygote: dm16:0 PE was 2.0 ± 0.16 mol%, dm18:0 PE was 0.40 ± 0.013 mol%, dm18:1n9 PE was 0.96 ± 0.012 mol%, and dm18:1n7 PE was 1.26 ± 0.063 mol% (n = 6 for each).

Sphingomyelinase activation at fertilization

SM can be hydrolyzed by sphingomyelinase to produce ceramide, and there is evidence that this enzyme is activated at fertilization. With the HPLC/ELSD method, a decrease of 230 pmol/cell in SM was found (**Fig. 7A**; Table 3) and, as measured by DAG kinase assay [for *Xenopus*, see (9)], ceramide levels increased 208 pmol/cell (Fig. 7B). Thus, we find a similar decrease of the substrate and increase in the product of sphingomyelinase and time course for these changes.

During fertilization, FA analysis finds a very large (53%) decrease in 18:1n9 SM (20.2 ± 1.0 mol% to 9.4 ± 0.2 mol%; $P < 0.02$; n = 3 each) (peak 13 in **Fig. 8**) and a small decrease in 22:1n9 (peak 32).

There were also significant increases in the SM species 16:0 (from 34.112 ± 0.798 mol% in the egg to 40.478 ± 0.478 mol% in the zygote; n = 3 each, $P < 0.009$) and two longer chain species: 24:0 (peak 38; 1.258 ± 0.111 mol% to 2.497 ± 0.210 mol%, n = 3 each, $P < 0.006$) and 24:1n9 (peak 39; 5.204 ± 0.429 mol% to 6.594 ± 0.278 mol%; n = 3 each, $P < 0.05$) (there was no significant change in peak 25, 20:2n6 SM; Fig. 8).

DAG levels during fertilization

In comparison with the differences in DAG noted between egg and sperm (Fig. 3), the egg and zygote values were similar (Table 2; **Fig. 9**). The major DAG species in the egg and the zygote are: 16:0 (peak 5), 18:1n9 (peak 13), and 22:1n9 (32). Reporting the difference in mass of DAG species (top panel, **Fig. 10**), there was an increase of 35 pmol/cell in 18:1n9 DAG and of 8 pmol/cell of 22:1n9 DAG during fertilization.

One way of searching for the source of DAG produced at fertilization (9) has been to compare changes in various phospholipid FAs with the change of those in DAG (58). Thus, the changes in the amount of DAG FAs during fer-

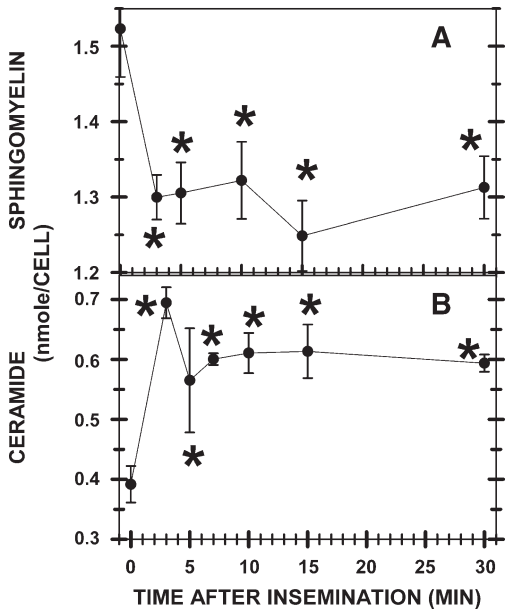

Fig. 7. Comparison of sphingomyelin (SM) and ceramide during fertilization. A: As measured by our HPLC method, SM decreased at fertilization. B: Ceramide, as measured with the enzymatic assay with DAG kinase, increased at fertilization. Asterisks denote significance at $P < 0.05$.

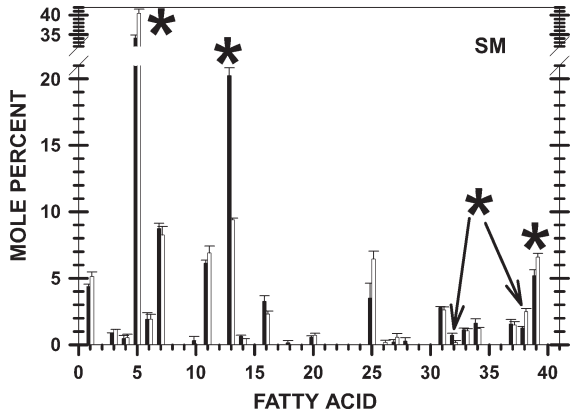

Fig. 8. Changes in SM FAs during fertilization. The first bar of the pair is the egg data, and the second is the zygote data. As noted for prior figures, the FAs are identified in Table 1. Asterisks denote significance at $P < 0.05$. Error bars indicate SEM.

tilization (top panel, Fig. 10) were compared with the changes in those of major phospholipids (bottom three panels of Fig. 10). In these three bottom panels, the change in the amount of each FA in the phospholipid classes (PC, PE, PI/PS) during fertilization was first calculated by subtracting the amount of each FA in the egg from that in the zygote. From this change in FAs during fertilization, the change in each FA in DAG was subtracted. When one looks at the lower panels in Fig. 10 for the shortest bars (which represent the least differences from the DAG increase), PC appears to be the closest, and thus PC may be the source of the DAG. More specifically, one can compare the 18:1n9 increase in DAG during fertilization (see top panel of Fig. 10) with the same peak in each of the lower three panels. For PC, there was only a small difference (0.021 nmol) from that for PE (0.907 nmol) or PI/PS (0.488 nmol). However, these data are open to other interpretations and DAG can be produced through multiple pathways (59, 60).

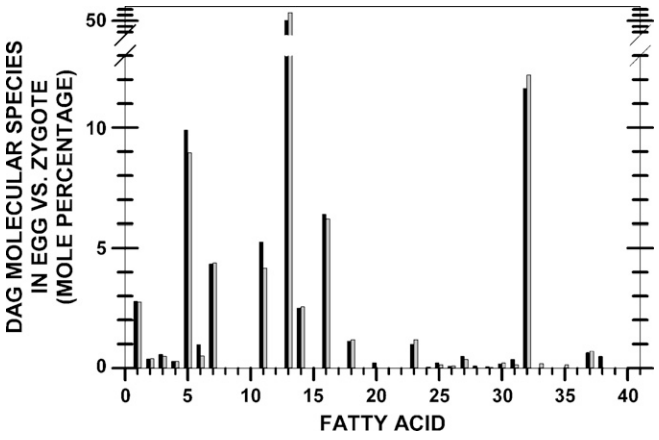

Fig. 9. The change in FAs of DAG during fertilization. The first bar of the pair is the egg data, and the second is the zygote data. Mole percent of each FA (identified in Table 1) refers to the amount of a FA in DAG, multiplied by 100 and divided by the total amount of all FAs in DAG.

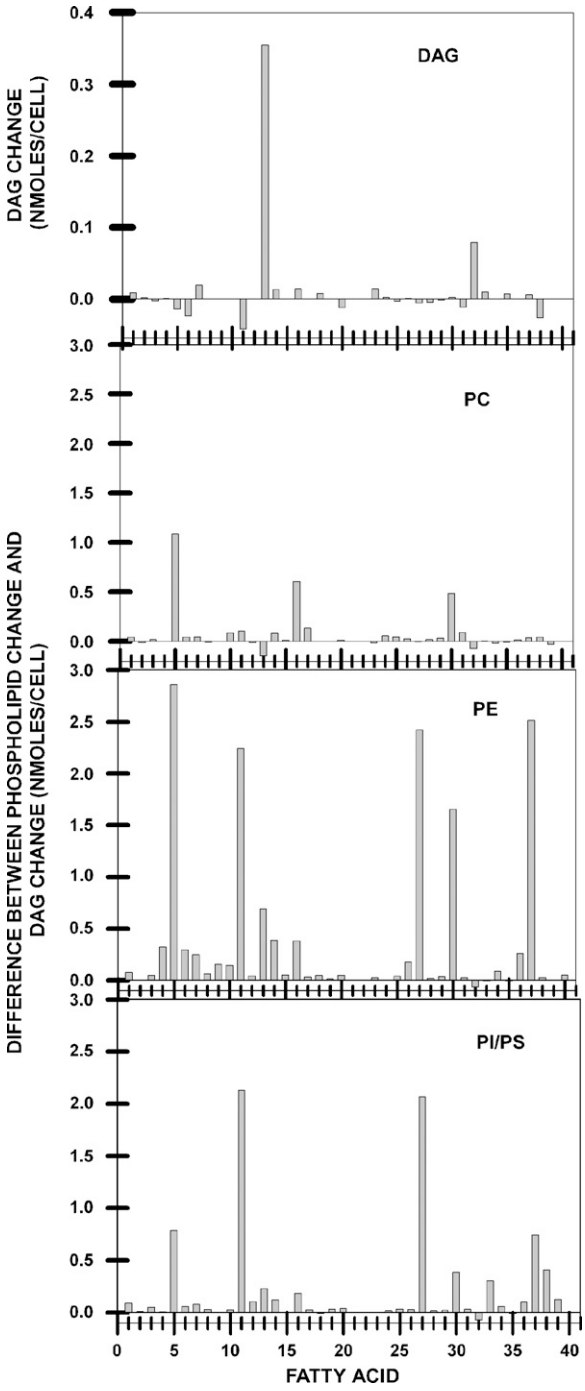

Fig. 10. Comparison of FAs from DAG and major phospholipids. To search for the source of the DAG increase at fertilization, the FAs from the elevated DAG and major phospholipid classes are compared. The top panel shows the change in FAs in DAG through fertilization and is the difference between the amount in the egg versus the zygote. An upward bar represents an increase in a DAG FA during fertilization. The lower three panels represent a comparison of the change in the phospholipid with the change in DAG during fertilization. The change in the amount of each FA in PC, PE, or PI/PS in the zygote was determined, and then the change in the amount of DAG (top panel) was subtracted. In the lower three panels, the panel showing the smallest bars would show which phospholipid has the fewest differences with the DAG increase and would represent a possible source for the DAG increase at fertilization.

DISCUSSION

We have now examined the following lipids during fertilization: IP3 (7, 8), DAG, choline, phosphocholine (9), and, from this report, DAG FA analysis, ceramide, SM, PC, LPC, PI, PE, PS, CL, and plasmalogens at fertilization (for summary, see Table 3).

Xenopus sperm and egg had very different lipid profiles, but they both undergo $[Ca^{2+}]_{in}$-induced exocytotic events and membrane fusion. We note that sperm had much higher levels of PE, PS, and SM, with much lower amounts of PC (PI was about the same; Figs. 1, 2). Similar to our high values of sperm SM (12 mol%; Fig. 2), Furland et al. (61) report higher than typical levels of SM (13–15 mol%) in bull and ram sperm and that SM may be required for a large production of ceramide during sperm capacitation. The high levels of SM may also reflect higher levels of rafts in sperm membranes.

When compared with *Xenopus* sperm (hatched bars, Fig. 2), Buhr, Curtis, and Somnapan Kakuda (62) found that boar sperm had lower PE (23 mol%), PI (3 mol%), PS (5 mol%), and higher PC (40 mol%) and SM (20 mol%).

In a pioneering lipid analysis of a plasma membrane-enriched fraction from sea urchin eggs by Kinsey, Decker, and Lennarz (63), unusually high levels of PI and PE were noted. In comparison, our analysis showed that PE (30 vs. 56 mol%), and PI (11 vs. 23 mol%) were lower in the *Xenopus* egg, whereas *Xenopus* PC was higher (55 vs. 16 mol%). No CL was detected in the sea urchin egg. Because the authors used purified KI-extracted cells and TLC methodology to analyze an enriched fraction of this invertebrate egg, many factors could explain the differences.

PLC activation at fertilzation

The major reaction of fertilization is considered to be the sperm-induced breakdown of PIP2 to IP3 and DAG through activation of PLC (46, 64–67). Although one would expect a decrease in PIP2, two reports show an increase in PIP2 during fertilization. First, PIP2 increases from 0.8 to 1.8 pmol of PIP2 per *Xenopus* egg/zygote during the first 10 min of fertilization (45). Second, presumably due to stimulation of PI 4 kinase by elevated calcium, there is an increase in PIP2 (as detected by an increased signal from a fluorescent PIP2 binding protein) during mouse fertilization (68). Kinsey and coworkers (64) report a 50% decline in PI in sea urchin fertilization and suggest that it is due to a replenishment of PIP2. A similar suggestion has been made (69) in regard to nuclear envelop reformation.

Consistent with prior work, we report a 32% decrease in total PI during *Xenopus* fertilization (1,172 pmol/cell; Fig. 4, Table 3). Thus, during *Xenopus* fertilization and activation of PLC, there might be a decrease in PI as PIP2 is regenerated through phosphorylation of PI and phosphatidylinositol 4-phosphate. Note that this PI decrease is 1,172-fold greater than the increase in PIP2, and this suggests that PI metabolism largely produces products other than PIP2 (perhaps phosphatidylinositol 3- or 4-phosphate). In addition to serving as a substrate for PLC, PIP2 may play many other roles, and the decrease in PI levels may produce active lipids other than PIP2. Finally, related to this discussion, if one assumes PIP2 levels of about 1 pmol per cell, and production of 0.173 pmol of IP3 (8) (Table 3), we estimate that only ~17% of PIP2 may be hydrolyzed at fertilization.

There were decreases in various FAs in the PI/PS fraction (e.g., 16:0, 16:1n7), but the largest declines were in 18:0 (~167 pmol/cell) and 18:1n9 (~352 pmol/cell). The latter FA, 18:1n9, decreased in LPC, PE, PI/PS, PC, and SM but increased in DAG (Fig. 5).

Both PI and, for the 3 min time point only, PS (234 pmol/cell) decrease (Fig. 4). Although PI and PS were examined together for FA analysis, the large change in total PI and the small, brief change in PS suggest that 18:0 and 18:1n9 may be the major species that decline in PI.

PLC prefers 18:0 at the *sn*-1 position and arachidonate 20:4n6 (and to a lesser extent, 22:5) in the *sn*-2 position of PIP2 (59, 69). These FAs would correspond to peaks 11, 27, 35, and 36 (the latter two for 22:5) in Fig. 5 for the PI/PS fraction. As noted above, there was a decrease in 18:0 in the PI/PS fraction, but the other FAs are either not detectable or do not decrease in this combined *Xenopus* phospholipid fraction.

Membrane phospholipid saturation and unsaturation

Wolf et al. (70) report both increases and decreases in membrane fluidity during fertilization and suggest that the results are due to different probes that lie in different membrane microdomains. Increasing saturation of phospholipids typically reduces membrane fluidity, but there were no detectable changes in saturation in CL, LPC, PC, or PE during fertilization (Fig. 6). The relative levels of saturation in the phospholipids were 1.0 CL, 2.15 LPC, 1.95 PC, 1.65 PE, 2.0 PS/PI, and 2.5 SM (Fig. 6). Thus, CL has the lowest level of saturation and SM has the highest.

In *Xenopus* eggs, the FA profile of LPC and SM were different from other major phospholipids in that they were predominately made up of saturated 16:0 and MUFA 18:1n9 with very low levels of PUFAs arachidonate 20:4n6, 20:5n3 EPA, and 22:6n3 DHA (Figs. 5, 8).

All phospholipids except CL showed a decline in the levels of MUFA during fertilization. In PI/PS, the levels of saturated and MUFA decreased by 10% and 17%, respectively, whereas PUFA increased 24%. *Xenopus* PLC is active at fertilization (7, 8, 46), and because PLC prefers tetraunsaturated PIP2 (59) and PIP2 is regenerated during fertilization, one might expect a decrease in PUFA in the combined PI/PS fraction.

PUFA levels did not change in CL, LPC, PC, or SM, but there was a small (7%) increase in PUFA in PE. Sperm, melanocytes, and nerve cells have high levels of PUFA (16, 36). The *Xenopus* egg averages ~40 mol% PUFA in the phospholipids CL, PC, PE, and PI/PS, whereas there is only ~13 mol% in LPC and SM.

The PUFA 22:6n3 (DHA) has been suggested to be a major regulator of membrane fluidity and raft structure, whereas high levels offer oxidation protection and can lead to apoptosis (16, 30, 36). In a comparison with other

FAs in all phospholipids, *Xenopus* eggs have a lower value of 9.4% of PUFA as 22:6n3, whereas silurid fish eggs contain 15–18% (71) and red blood cells contain 4% (16). Considering the amount of 22:6n3 in *Xenopus* egg CL, LPC, PC, PE, PS/PI, and SM, about 93% of 22:6n3 is found in PC (65%) and PE (27%), whereas all of the other phospholipids contain very small amounts. There were no changes in 22:6n3 PC or 22:6n3 PE during fertilization; however, 22:6n3 LPC increased over 2-fold (Fig. 5).

The long, saturated FA tail of SM stabilizes rafts. Thus, the increase in saturation (19%) and the decrease in MUFA (30%) SM could represent a stabilization of rafts during fertilization. However, as noted, there is also a decrease in the amount of SM to produce ceramide, and this could represent a destabilization of rafts (although ceramide can stabilize rafts). Perhaps the increase in SM saturation is a method to stabilize rafts in the presence of decreased SM.

LPC changes in fertilization

There are relatively few major species of *Xenopus* egg LPC and most are less than 18 carbons long or less: 16:0, *trans*-16:1n7, 18:0, and 18:1n9 (Fig. 5).

The 50% decrease in total LPC during fertilization might reflect the activation of an enzyme such as autotaxin. Autotaxin is a lysophospholipase D that catalyzes the hydrolysis of LPC to lysophosphatidic acid (74). Lysophosphatidic acid is a well-known signaling lipid that binds to G protein-coupled receptors to release calcium but also may have intracellular action (19).

As noted earlier, PLA2 inhibition blocks some fertilization events, and there is evidence that LPC, produced through the action of PLA2 on PC, plays a role in membrane fusion (20, 21). Although this should be examined directly, the ~50% drop in total amount LPC during fertilization suggests that high levels of LPC do not play a role in sperm-egg fusion or subsequent cortical granule exocytosis.

However, the increase in DHA 22:6n3 LPC during fertilization (Fig. 5) could facilitate membrane fusion and represent an activation of PLA2. There was no detectable decrease in 22:6n3 PC (10.523 ± 0.150 mol% to 10.036 ± 0.274 mol%; $P < 0.19$; peak 37 in Fig. 5), although the large amount of this species could obscure small changes.

Mammalian PLA2 is believed to act through release of arachidonic acid (20:4n6) from PC, and arachidonate can have effects on *Xenopus* cells (72). During fertilization, there was no detectable change in the 20:4n6 arachidonate species of CL, LPC, PC, PS/PI, or SM (arachidonate PE actually increased; Fig. 5). PLA2 may be able to break down the plasmalogen form of PC (e.g., 73), but there was no detectable change in this species during fertilization. Further work is needed to directly examine whether decreased LPC, lysophosphatidic acid, arachidonate release, PLA2, or autotaxin plays a role in fertilization.

Phospholipid changes

Although the total level of PC did not significantly change during fertilization, there was a decrease in 18:1n9 species of PC from 12.7 to 12.3 mol% (estimated as an increase of ~430 pmol/cell) (Fig. 5). In addition to any PLA2 activation (see discussion above), PLD activation at fertilization would degrade PC to PA and choline, and any PA produced at fertilization should reflect the FA species of PC. To lend support for an activation of PLD during fertilization, we have reported a 134 pmol/cell increase in choline mass during *Xenopus* fertilization (Table 3) (9).

At fertilization, there was no detectable change in total PE mass, but there was a decrease in 18:1n9 and an increase in the arachidonate and EPA species in PE [DHA PE showed a trend toward an increase, $P < 0.08$; (Fig. 5)]. As noted for phosphoinositides, there may be a hydrolysis and subsequent synthesis of PE during fertilization.

Note that addition of 20:5n3 EPA to cancer cells has been found to remove SM and cholesterol from rafts, increase ceramide in rafts, and induce apoptosis (30). However, there were no decreases in any phospholipid EPA, so there is no support for a release of this FA at fertilization (peak 30; Fig. 5). As noted, EPA increased during fertilization in PE and PS/PI.

Because CL may play a role in membrane fusion (25–29), we note that total CL did not change during fertilization, so this does not provide support for elevated CL producing sperm-egg fusion or cortical granule exocytosis. However, there was a decrease in 16:1n7, and increases in *trans*-18:1n9 and 20:0 (Fig. 5) that may relate to a role for CL in fertilization. CL was very unusual in that it contained very large amounts (~22 mol%) of 22:2n6 (peak 33; Fig. 5) and low levels of arachidonate, EPA, and DHA. All other phospholipids contained only trace amounts, up to ~2 mol% 22:2N6.

Plasmalogens

Plasmalogens have been implicated as crucial to survival of sperm owing to their antioxidant properties (22, 23). Furthermore, plasmalogens may raise membrane fluidity and play a role in membrane fusion (69). Not surprisingly, sperm have relatively high levels of plasmalogens (22, 23). As compared with *Xenopus* eggs, there appears to be more sperm plasmalogen dm16:0 (peak 4, Fig. 3) and dm18:1n9 DAG (peak 9), because these plasmalogens were not detectable in eggs. There were no detectable changes in plasmalogen species during fertilization.

In comparison to other animal tissues, the relative amounts of plasmalogens found in the *Xenopus* egg were typical, in that they were present at low levels, predominately in PE, with lower levels in PC (little or none found in PI or PS) (22). Total *Xenopus* PE plasmalogens were 4.7-fold greater than those from PC. The relative amount of PC plasmalogens was dm16:0 (0.16 mol%) > dm18:1n7 (0.08 mol%) >> dm18:0 and dm18:1n9, and for those in PE, dm16:0 (~2 mol%) > dm18:1n7 (~1.3 mol%) > dm18:1n9 (0.98 mol%) > dm18:0 (0.4 mol%).

Highly fusogenic vesicles from sea urchin egg cytoplasm contain PC that is almost exclusively plasmalogen, with especially high levels of dm18:1/20:5 (12 mol%), dm18:0/20:5 (20 mol%), and dm18:0/22:6 PC (15 mol%) (69). *Xenopus* egg PC also has a relatively high amount of dm18:1n7 and 20:5n3 EPA (7.72 mol%; compare peak

30 with others in Fig. 5, top panel). Perhaps of interest, *Xenopus* egg PE has a relatively high mole percent of these two species.

SM and ceramide

We find evidence that sphingomyelinase is activated at fertilization, because there was an equivalent decrease in total SM and increase in ceramide (~220 pmol/cell) (Table 3) and similar time course for change (Fig. 7). Because 18:1n9 SM declined by 53% (Fig. 8), any activation of a *Xenopus* sphingomyelinase at fertilization might prefer this substrate, and the ceramide produced would reflect this species. As noted, SM shows the highest level of saturation and the lowest (3-fold lower) percentage of PUFAs of the major phospholipids. During fertilization, there was an increase in saturated FAs and a decrease in MUFAs in SM.

During fertilization, ceramide increased from 392 to 600 pmol per egg or zygote (Fig. 7; Table 3). Similarly, Coll et al. (75) report the basal level of ceramide in *Xenopus* oocytes as ~200 pmol/oocyte, and artificial production of ceramide maximizes at ~800 pmol/oocyte.

One might expect that the SM decrease in fertilization would lead to the breakdown of membrane rafts, increased membrane disorder (76–78), and inhibition of secretory vesicle fusion (31). However, functional rafts are present during fertilization (46), and cortical granule exocytosis proceeds during this decrease in SM. Perhaps the increase in saturation and decrease in MUFA SM ameliorate any negative effects of a decrease in total SM.

The increase in ceramide during fertilization is surprising, inasmuch as the lipid is typically associated with increased apoptosis in eggs (41). The early embryo is resistant to ceramide-induced apoptosis (42), so ceramide presumably would have functions other than induction of apoptosis. Ceramide stabilizes membrane rafts (79) and alters PKC activity (59, 80). Ceramide could be metabolized to sphingosine and sphingosine-1-phosphate, and both have been found to release $[Ca++]_{in}$ (81). Addition of ceramide to mammalian sperm enhanced exocytosis (e.g., the acrosome reaction) (37, 38, 82), but we were unable to find any references linking ceramide (or sphingomyelinase or SM) and fertilization. Preliminary experiments with a neutral sphingomyelinase inhibitor (GW4869) found that the drug did not inhibit fertilization.

It is interesting that the addition of ceramide to *Xenopus* oocytes induces meiosis (75) and that one event of fertilization is the completion of meiosis. Furthermore, ceramide addition to *Xenopus* oocytes released $[Ca^{2+}]_{in}$ through Gq, PLCβ, and IP3 receptor activation (83). Because this G protein pathway is not thought to be involved in $[Ca^{2+}]_{in}$ release as initiated by sperm (84), ceramide may not play a role in the calcium release at fertilization. However, understanding sphingomyelinase activation and the role of ceramide during fertilization requires further study.

DAG levels

Relative to eggs, DAG levels in sperm appeared to contain more 16:0, *trans*-16:1n7, 18:0, arachidonate 20:4n6, and plasmalogen dm18:1n9 (Fig. 3). Because the primary functions of sperm are to move and fuse with the egg, these lipid levels may relate to these or other functions (e.g., enzyme activation, protection against lipid oxidation).

DAG 18:0/20:4n6 is very high during fusion of vesicles around sperm DNA that has just entered the egg/zygote cytoplasm after fertilization, and has been implicated in membrane fusion in other cells (52, 69, 85). As noted above, higher levels of these FAs in DAG are present in *Xenopus* sperm, so they may play a role in the acrosome reaction (membrane fusion of the acrosome) or in sperm-egg fusion.

Source of DAG increase during fertilization

Based on our prior measurement of IP3, there should be a small (173 fmol/cell), rapid (5 min or less after insemination) increase in DAG that derives from PIP2 hydrolysis by PLC (7–9). The molecular species of this DAG increase should reflect that of PIP2 and PI (59). We report that *sn*-1,2-DAG activated PKC α and β translocated to the plasma membrane by 7–10 min after insemination (9). However, with basal *sn*-1,2-DAG in *Xenopus* eggs at 62 pmol, it is difficult to detect the small DAG increase.

Elevated levels of arachidonate 20:4n6 DAG during membrane fusion are believed to be due to production by PLCγ in the fusogenic vesicles (69, 85). That is, 20:4n6 DAG derives from PIP2 (see earlier discussion of PLC specificity), not PC. Because PI molecular species reflect PIP2 species, note that the two highest levels of FAs in *Xenopus* egg PI/PS are 18:0 and 20:4n6 (Fig. 5). The mole percent of 18:0 or 20:4n6 in PI/PS is higher than that in PC, CL, PE, or LPC (Fig. 5). Thus, although we were unable to detect any change in the small amount of arachidonate DAG during fertilization, DAG containing 20:4n6 may be produced from PIP2 hydrolysis (as noted, we would not expect to see a change of 0.173 fmol/cell based on the change in IP3 mass).

The late (12 min), larger 48 pmol/cell increase in DAG at fertilization is easily measurable, inasmuch as it is ~300-fold larger than the IP3 increase at fertilization (9). Based on data presented in Fig. 10, this larger DAG increase may be derived from PC hydrolysis. Some 80% of the increase in the large, late DAG during fertilization was due to 18:1n9, whereas 22:1n9 contributed another ~17% (Fig. 10, top panel). These data suggest that the DAG increase of 48 pmol/cell during fertilization (which was measured with a DAG kinase assay; Table 3) (9) is due to increases in these two species of DAG (measured with gas chromatography). There is support for this suggestion because the size of the increase of 18:1n9 was 35 pmol and 22:1n9 was 8 pmol, for a total of 43 pmol.

The molecular species of DAG derived from PIP2 is largely made up of highly polyunsaturated FAs (e.g., 20:4 and 22:6), whereas that from PC is made up of saturated and monounsatured FAs (3, 59, 85). Thus, because the large, late DAG increase at fertilization is due to monounsaturated DAG (e.g., 18:1n9 and 22:1n9), there is further evidence that it derives from PC.

If this large 48 pmol increase in DAG was produced through PLC hydrolysis of PIP2, one might expect more PIP2 present during *Xenopus* fertilization (~1 pmol/cell) (45). Further support for the large DAG increase deriving from PC, not PIP2, hydrolysis is the timing: we found that the IP3 (and thus, PIP2-derived DAG) production peak was much earlier (5 min) than that of the larger DAG (~12 min). Many other cellular systems have a DAG production from the breakdown of PIP2 that is much faster and smaller than that of DAG production from PC (60).

The 20,000 pmol of PC present in a *Xenopus* egg (Fig. 4) is obviously sufficient to produce the late, large DAG increase. More specifically, we showed that the only detectable change in PC FAs at fertilization was a decrease in the amount of 18:1n9 (peak 13; Fig. 5), the same FA that increases in DAG (peak 13; Figs. 9, 10, top panel). The decrease in 18:1n9 PC was estimated as ~430 pmol/cell, and this is ~9-fold larger than the 48 pmol increase in DAG. This difference may mean that DAG is not from this species of PC, that data are inaccurate, or that other lipases (e.g., PLD) also degrade this species of PC. 18:1n9 PI/PS, PE, and LPC also show a decrease of about 220–310 pmol/cell and could be sources of the late DAG increase at fertilization. However, Wakelam (59) suggests that reports on PE or PI hydrolysis to DAG are unconfirmed, or if real, represent unusual circumstances.

PKC is believed to be important in fertilization (47–50), but the type of DAG is important for PKC activation. DAG that derives from PC hydrolysis may not stimulate PKC, because this DAG is typically made up of saturated fatty acids or MUFAs, and DAGs made up of these species are unable to stimulate PKC (58, 59, 86, 87; however, see 88). Thus, the late, large monounsaturated DAG fertilization increase may not stimulate *Xenopus* PKC but may play other roles (perhaps aiding membrane fusion in the massive cortical granule exocytosis that occurs at ~7–13 min postfertilization).

In summary, this examination of the total amount and FA composition of the major lipid classes closes gaps that exist in the fertilization literature. These lipidomic data provide baseline values that will aid in developing a more comprehensive model of fertilization. Relative amounts of lipids in sperm, eggs, and zygotes are important for understanding gamete physiology, the role of rafts, and the events of fertilization. We report levels of species of DAG, the major classes of phospholipids, CL, LPC, plasmalogens, and sphingolipids (including SM and ceramide). We found a decrease in total LPC, SM, and PI and suggest that phosphorylation of PI leads to higher levels of PIP2 during fertilization. There were changes in MUFA and PUFA associated with fertilization. We report an increase in ceramide and the FA species of DAG during fertilization. With the data presented here, further studies on PLA2, PLD, autotoxin, and sphingomyelinase are warranted.

The authors thank students Thomas E. Morrison, Cheney Lupe, Patricia Medina, Pablo Joucovsky, Carolyn Anello, Erinn Stauter, Liliana Cabrera, David Carujo, Stephen Sharp, Crystal Szczesny, Cassandra Shum, Elizabeth Lampert, Ingar Krebs, and Ryan Koonze.

REFERENCES

1. Dennis, E. A., H. A. Brown, R. Deems, C. K. Glass, A. H. Merrill, R. C. Murphy, C. R. H. Raetz, W. Shaw, S. Subramaniam, and D. W. Russell. 2006. The LIPID MAPS approach to lipidomics. *In* Functional Lipidomics. L. Feng and G. D. Prestwich, editors. CRC Press/Taylor and Francis Group, Boca Raton, FL. 1–15.
2. Feng, L., and G. D. Prestwich, editors. 2006. Functional Lipidomics. CRC Press/Taylor and Francis Group, Boca Raton, FL.
3. Brose, N., and C. Rosenmund. 2002. Move over protein kinase C, you've got company: alternative cellular effectors of diacylglycerol and phorbol esters. *J. Cell Sci.* **115:** 4399–4411.
4. Martelli, A. M., F. Falà, I. Faenza, A. M. Billi, A. Cappellini, L. Manzoli, and L. Cocco. 2004. Metabolism and signaling activities of nuclear lipids. *Cell. Mol. Life Sci.* **61:** 1143–1156.
5. Wang, J., Megha, and E. London. 2004. Relationship between sterol/steroid structure and participation in ordered lipid domains (lipid rafts): implications for lipid raft structure and function. *Biochemistry.* **43:** 1010–1018.
6. Stith, B. J., C. Jaynes, M. Goalstone, and S. Silva. 1992. Insulin and progesterone increase ^{32}PO4-labeling of phospholipids and inositol 1,4,5-trisphosphate mass in *Xenopus* oocytes. *Cell Calcium.* **5:** 341–352.
7. Stith, B. J., M. Goalstone, S. Silva, and C. Jaynes. 1993. Inositol 1,4,5-trisphosphate mass changes from fertilization through first cleavage in *Xenopus laevis*. *Mol. Biol. Cell.* **4:** 435–443.
8. Stith, B. J., R. Espinoza, D. Roberts, and T. Smart. 1994. Sperm increase inositol 1,4,5-trisphosphate mass in *Xenopus laevis* eggs preinjected with calcium buffers or heparin. *Dev. Biol.* **165:** 206–215.
9. Stith, B. J., K. Woronoff, R. Espinoza, and T. Smart. 1997. sn-1,2-Diacylglycerol and choline increase after fertilization in *Xenopus laevis*. *Mol. Biol. Cell.* **4:** 755–765.
10. Witte, T. S., and S. Schäfer-Somi. 2007. Involvement of cholesterol, calcium and progesterone in the induction of capacitation and acrosome reaction of mammalian spermatozoa. *Anim. Reprod. Sci.* **102:** 181–193.
11. Tsaadon, A., E. Eliyahu, N. Shtraizent, and R. Shalgi. 2006. When a sperm meets an egg: block to polyspermy. *Mol. Cell. Endocrinol.* **252:** 107–114.
12. Liang, C. G., Y. Q. Su, H. Y. Fan, H. Schatten, and Q. Y. Sun. 2007. Mechanisms regulating oocyte meiotic resumption: roles of mitogen-activated protein kinase. *Mol. Endocrinol.* **21:** 2037–2055.
13. Visconti, P. E., V. A. Westbrook, I. Chertihin, I. Dmarco, S. Sleight, and A. B. Dickman. 2002. Novel signaling pathways involved in sperm acquisition of fertilizing capacity. *J. Reprod. Immunol.* **53:** 133–150.
14. Gomathi, C., K. Balasubramanian, N. V. Bhanu, V. Srikanth, and P. Govindarajulu. 1993. Effect of chronic alcoholism on semen—studies on lipid profiles. *Int. J. Androl.* **16:** 175–181.
15. Blesbois, E., I. Grasseau, and D. Hermier. 1999. Changes in lipid content of fowl spermatozoa after liquid storage at 2 to 5 degrees C. *Theriogenology.* **52:** 325–334.
16. Lenzi, A., M. Picardo, L. Gandini, and F. Dondero. 1996. Lipids of the sperm plasma membrane: from polyunsaturated fatty acids considered as markers of sperm function to possible scavenger therapy. *Hum. Reprod. Update.* **2:** 246–256.
17. Feki, N. C., P. Thérond, M. Couturier, G. Liméa, A. Legrand, P. Jouannet, and J. Auger. 2004. Human sperm lipid content is modified after migration into human cervical mucus. *Mol. Hum. Reprod.* **10:** 137–142.
18. Liguori, L., E. de Lamirande, A. Minelli, and C. Gagnon. 2005. Various protein kinases regulate human sperm acrosome reaction and the associated phosphorylation of Tyr residues and of the Thr-Glu-Tyr motif. *Mol. Hum. Reprod.* **11:** 211–221.
19. Meyer zu Heringdorf, D., and K. H. Jakobs. 2007. Lysophospholipid receptors: signaling, pharmacology and regulation by lysophospholipid metabolism. *Biochim. Biophys. Acta.* **1768:** 923–940.
20. Kamata, Y., M. Mita, A. Fujiwara, T. Tojo, J. Takano, A. Ide, and I. Yasumasu. 1997. Probable participation of phospholipase A2 reaction in the process of fertilization-induced activation of sea urchin eggs. *Dev. Growth Differ.* **39:** 419–428.
21. Riffo, M. S., and M. Parraga. 1997. Role of phospholipase A2 in

mammalian sperm-egg fusion: development of hamster oolemma fusibility by lysophosphatidylcholine. *J. Exp. Zool.* **279:** 81–88.
22. Reisse, S., G. Rothardt, A. Volkl, and K. Beier. 2001. Peroxisomes and ether lipid biosynthesis in rat testis and epididymus. *Biol. Reprod.* **64:** 1689–1694.
23. Gorgas, K., and A. Teigler, D. Komljenovic, and W. W. Just. 2006. The ether lipid-deficient mouse: tracking down plasmalogen functions. *Biochim. Biophys. Acta.* **1763:** 1511–1526.
24. Gennis, R. B. 1989. Biomembranes: Molecular Structure and Function. Springer-Verlag, New York.
25. Ortiz, A., J. Killian, A. Verkleij, and J. Wilschut. 1999. Membrane fusion and the lamellar-to-inverted-hexagonal phase transition in cardiolipin vesicle systems induced by divalent cations. *Biophys. J.* **77:** 2003–2014.
26. Arts, E. G., J. Kuiken, S. Jager, and D. Hoekstra. 1993. Fusion of artificial membranes with mammalian spermatozoa. Specific involvement of the equatorial segment after acrosome reaction. *Eur. J. Biochem.* **217:** 1001–1009.
27. Geva, E., A. Amit, L. Lerner-Geva, Y. Yaron, Y. Daniel, T. Schwartz, F. Azem, I. Yovel, and J. B. Lessing. 2000. Prednisone and aspirin improve pregnancy rates in patients with reproductive failure and autoimmune antibodies: a prospective study. *Am. J. Reprod. Immunol.* **43:** 36–40.
28. Ulcova-Gallova, Z. 2005. Antiphospholipid antibodies and reproductive failure. *Chem. Immunol. Allergy.* **88:** 139–149.
29. Bearer, E. L., and D. S. Friend. 1982. Modifications of anionic-lipid domains preceding membrane fusion in guinea pig sperm. *J. Cell Biol.* **92:** 604–615.
30. Schley, P. D., D. N. Brindley, and C. J. Field. 2007. (n-3) PUFA alter raft lipid composition and decrease epidermal growth factor receptor levels in rafts of human breast cancer cells. *J. Nutr.* **137:** 548–553.
31. Rogasevskaia, T., and J. R. Cootssen. 2006. Sphingomyelin-enriched microdomains define the efficiency of native Ca^{2+}-triggered membrane fusion. *J. Cell Sci.* **119:** 2688–2694.
32. Luria, A., V. Vegelyte-Avery, B. Stith, N. M. Tsvetkova, W. F. Wolkers, J. H. Crowe, F. Tablin, and R. Nuccitelli. 2002. Discrete microdomains in the plasma membrane of *Xenopus laevis* eggs. *Biochemistry.* **41:** 13189–13197.
33. Sato, K-I., A. A. Tokmakov, T. Iwasaki, and Y. Fukami. 2000. Tyrosine kinase-dependent activation of phospholipase Cγ is required for calcium transient in *Xenopus* egg fertilization. *Dev. Biol.* **224:** 453–469.
34. Sato, K-I., A. A. Tokmakov, C-L. He, M. Kurokawa, T. Iwasaki, M. Shirouzu, R. A. Fissore, S. Yokoyama, and Y. Fukami. 2003. Reconstitution of Src-dependent phospholipase Cγ phosphorylation and transient calcium release by using membrane rafts and cell-free extracts from *Xenopus* eggs. *J. Biol. Chem.* **278:** 38413–38420.
35. Sakakibara, K., K. Sato, K. Yoshino, N. Oshiro, S. Hirahara, A. K. Mahbub Hasan, T. Iwasaki, Y. Ueda, Y. Iwaw, K. Yonezawa, et al. 2005. Molecular identification and characterization of *Xenopus* egg uroplakin III, an egg raft-associated transmembrane protein that is tyrosine-phosphorylated upon fertilization. *J. Biol. Chem.* **280:** 15029–15037.
36. Lessig, J., C. Gey, R. Suss, J. Schiller, H-J. Glander, and J. Arnhold. 2004. Analysis of the lipid composition of human and boar spermatozoa by MALDI-TOF mass spectrometry, thin layer chromatography, and P31 NMR spectroscopy. *Comp. Biochem. Physiol. B Biochem. Mol. Biol.* **137:** 265–277.
37. Murase, T., N. Imaeda, N. Kondown, and T. Tsubota. 2004. Ceramide enhances acrosome exocytosis triggered by calcium and the calcium ionophore A23187 in boar spermatozoa. *J. Reprod. Dev.* **50:** 667–674.
38. Cross, N. L. 2000. Sphingomyelin modulates capacitation of human sperm in vitro. *Biol. Reprod.* **63:** 1129–1134.
39. Marston, J. H., and M. C. Chang. 1964. The fertilizable life of ova and their morphology following delayed insemination in mature and immature mice. *J. Exp. Zool.* **155:** 237–252.
40. Tilly, J. L., and R. N. Kolesnick. 2002. Sphingolipids, apoptosis, cancer treatments and the ovary: investigating a crime against female fertility. *Biochim. Biophys. Acta.* **1585:** 135–138.
41. Perez, G. I., A. Jurisicova, T. Matikainen, T. Monyama, M. R. Kim, Y. Takai, J. K. Pru, R. N. Kolesnick, and J. L. Tilly. 2005. A central role for ceramide in the age-related acceleration of apoptosis in the female germline. *FASEB J.* **19:** 860–862.
42. Savtchouk, I. A., F. J. Mattie, and A. A. Ollis. 2007. Ceramide: from embryos to tumors. *Sci. STKE.* **394:** jc1.
43. Eliyahu, E., J. H. Park, N. Shtraizent, X. He, and E. H. Schuchman. 2007. Acid ceramidase is a novel factor required for early embryo survival. *FASEB J.* **21:** 1403–1409.
44. Otala, M., M. O. Pentikäinen, T. Matikainen, L. Suomalainen, J. K. Hakala, G. I. Perez, M. Tenhunen, K. Erkkilä, P. Kovanen, M. Parvinen, et al. 2005. Effects of acid sphingomyelinase deficiency on male germ cell development and programmed cell death. *Biol. Reprod.* **72:** 86–96.
45. Snow, P., D. L. Yim, J. D. Leibow, S. Saini, and R. Nuccitelli. 1996. Fertilization stimulates an increase in inositol trisphosphate and inositol lipid levels in *Xenopus* eggs. *Dev. Biol.* **180:** 108–118.
46. Sato, K-I., Y. Fukami, and B. J. Stith. 2006. Signal transduction pathways leading to Ca^{2+} release in vertebrate fertilization: lessons from *Xenopus* eggs. *Semin. Cell Dev. Biol.* **17:** 285–292.
47. Vasilets, L. A., G. Schmalzing, K. Mädefessel, W. Haase, and W. Schwarz. 1990. Activation of protein kinase C by phorbol ester induces downregulation of the Na+/K(+)-ATPase in oocytes of *Xenopus laevis*. *J. Membr. Biol.* **118:** 131–142.
48. Khan, N. A., V. Quemener, and J. P. Moulinoux. 1991. Exogenous diacylglycerols downregulate the activity of Na(+)-K+ pump in *Xenopus laevis* oocytes. *Exp. Cell Res.* **194:** 248–251.
49. Bement, W. M., and D. G. Capco. 1989. Activators of protein kinase C trigger cortical granule exocytosis, cortical contraction, and cleavage furrow formation in *Xenopus laevis* oocytes and eggs. *J. Cell Biol.* **108:** 885–892.
50. Gundersen, C. B., S. A. Kohan, Q. Chen, J. Iagnemma, and J. A. Umbach. 2002. Activation of protein kinase Cε triggers cortical granule exocytosis in *Xenopus* oocytes. *J. Cell Sci.* **115:** 1313–1320.
51. Swann, K., D. H. McCulloh, A. McDougall, E. L. Chambers, and M. Whitaker. 1992. Sperm-induced currents at fertilization in sea urchin eggs injected with EGTA and neomycin. *Dev. Biol.* **151:** 552–563.
52. Barona, T., R. D. Byrne, T. R. Pettitt, M. J. O. Wakelam, B. Larijani, and D. L. Poccia. 2005. Diacylglycerol induces fusion of nuclear envelope membrane precursor vesicles. *J. Biol. Chem.* **280:** 41171–41177.
53. Pai, J. K., J. A. Pachter, I. B. Weinstein, and W. R. Bishop. 1991. Overexpression of protein kinase Cβ1 enhances phospholipase D activity and diacylglycerol formation in phorbol ester-stimulated rat fibroblasts. *Proc. Natl. Acad. Sci. USA.* **88:** 598–602.
54. Stith, B. J., J. Hall, P. Ayes, L. Waggoner, J. Moore, and W. Shaw. 2000. Quantification of major classes of *Xenopus* phospholipids. *J. Lipid Res.* **41:** 1448–1454.
55. Watkins, S. M., T. Y. Lin, R. M. Davis, J. R. Ching, E. J. DePeters, G. M. Halpern, R. L. Walzem, and J. B. German. 2001. Unique phospholipid metabolism in mouse heart in response to dietary docosahexaenoic or alpha-linolenic acids. *Lipids.* **36:** 247–254.
56. Preiss, J., C. R. Loomis, W. R. Bishop, R. Stein, J. E. Niedel, and R. M. Bell. 1986. Quantitative measurement of sn-1,2-diacylglycerols present in platelets, hepatocytes, and ras- and sis-transformed normal rat kidney cells. *J. Biol. Chem.* **261:** 8597–8600.
57. Stith, B. J., A. J. Kirkwood, and E. Wohnlich. 1991. Insulin-like growth factor 1, insulin and progesterone induce early and late increases in *Xenopus* oocyte sn-1,2-diacylglycerol levels before meiotic cell division. *J. Cell. Physiol.* **149:** 252–259.
58. Leach, K. L., V. A. Ruff, T. M. Wright, M. S. Pessin, and D. M. Raben. 1991. Dissociation of protein kinase C activation and sn-1,2-diacylglycerol formation. Comparison of phosphatidylinositol- and phosphatidylcholine-derived diglycerides in alpha-thrombin-stimulated fibroblasts. *J. Biol. Chem.* **266:** 3215–3221.
59. Wakelam, M. J. O. 1998. Diacylglycerol—when is it an intracellular messenger? *Biochim. Biophys. Acta.* **1436:** 117–126.
60. Griner, E. M., and M. G. Kazanietz. 2007. Protein kinase C and other diacylglycerol effectors in cancer. *Nat. Rev. Cancer.* **7:** 281–294.
61. Furland, N. E., S. R. Zanetti, G. M. Oresti, E. N. Maldonado, and M. I. Aveldaño. 2007. Ceramides and sphingomyelins with high proportions of very long-chain polyunsaturated fatty acids in mammalian germ cells. *J. Biol. Chem.* **282:** 18141–18150.
62. Buhr, M. M., E. F. Curtis, and N. Somnapan Kakuda. 1994. Composition and behavior of head membrane lipids of fresh and cryopreserved boar sperm. *Cryobiology.* **31:** 224–238.
63. Kinsey, W. H., G. L. Decker, and W. J. Lennarz. 1980. Isolation and partial characterization of the plasma membrane of the sea urchin egg. *J. Biol. Chem.* **87:** 248–254.
64. Kamel, L. C., J. Bailey, L. Schoenbaum, and W. Kinsey. 1985. Phosphatidylinositol metabolism during fertilization in the sea urchin egg. *Lipids.* **20:** 350–356.
65. Picard, A., F. Giraud, F. Le Bouffant, F. Sladeczek, C. Le Peuch, and M. Dorée. 1985. Inositol 1,4,5-triphosphate microinjection triggers activation, but not meiotic maturation in amphibian and starfish oocytes. *FEBS Lett.* **182:** 446–450.

66. Sillers, P. J., and A. Forer. 1985. Ca++ in fertilization and mitosis: the phosphatidylinositol cycle in sea urchin gametes and zygotes is involved in control of fertilization and mitosis. *Cell Biol. Int. Rep.* **9:** 275–282.
67. Busa, W. B., and R. Nuccitelli. 1985. An elevated free cytosolic Ca2+ wave follows fertilization in eggs of the frog, *Xenopus laevis*. *J. Cell Biol.* **100:** 1325–1329.
68. Halet, G., R. Tunwell, T. Balla, K. Swann, and J. Carroll. 2002. The dynamics of plasma membrane PtdIns(4,5)P(2) at fertilization of mouse eggs. *J. Cell Sci.* **115:** 2139–2149.
69. Byrne, R. D., T. M. Barona, M. Garnier, G. Koster, M. Katan, D. L. Poccia, and B. Larijani. 2005. Nuclear envelope assembly is promoted by phosphoinositide-specific phospholipase C with selective recruitment of phosphatidylinositol-enriched membranes. *Biochem. J.* **387:** 393–400.
70. Wolf, D. E., W. Kinsey, W. Lennarz, and M. Edidin. 1981. Changes in the organization of the sea urchin egg plasma membrane upon fertilization: indications from the lateral diffusion rates of lipid-soluble fluorescent dyes. *Dev. Biol.* **81:** 133–138.
71. Mukhopadhyay, T., and S. Ghosh. 2007. Lipid profile and fatty acid composition of two silurid fish eggs. *J. Oleo Sci.* **56:** 399–403.
72. Carattino, M. D., W. G. Hill, and T. R. Kleyman. 2003. Arachidonic acid regulates surface expression of epithelial sodium channels. *J. Biol. Chem.* **278:** 36202–36213.
73. Davis, B., G. Koster, L. J. Douet, M. Scigelova, G. Woffendin, J. M. Ward, A. Smith, J. Humphries, K. G. Burnand, C. H. Macphee, et al. 2008. Electrospray ionization mass spectrometry identifies substrates and products of lipoprotein-associated phospholipase A2 in oxidized human low density lipoprotein. *J. Biol. Chem.* **383:** 6428–6437.
74. van Meeteren, L. A., and W. H. Moolenaar. 2007. Regulation and biological activities of the autotaxin-LPA axis. *Prog. Lipid Res.* **46:** 145–160.
75. Coll, O., A. M. Morales, J. C. Fernandez-Checa, and C. Garcia-Ruiz. 2007. Neutral sphingomyelinase-induced ceramide triggers germinal vesicle breakdown and oxidant-dependent apoptosis in *Xenopus laevis* oocytes. *J. Lipid Res.* **48:** 1924–1935.
76. Anderson, R. G., and K. Jacobson. 2002. A role for lipid shells in targeting proteins to caveolae, rafts, and other lipid domains. *Science.* **296:** 1821–1825.
77. Edidin, M. 2003. The state of lipid rafts: from model membranes to cells. *Annu. Rev. Biophys. Biomol. Struct.* **32:** 257–283.
78. Aida, E., F. Cremestia, M. Gonib, and R. Kolesnick. 2002. Role of sphingomyelinase and ceramide in modulating rafts: do biophysical properties determine biologic outcome? *FEBS Lett.* **531:** 47–53.
79. Sot, J., L. A. Bagatolli, F. M. Goñi, and A. Alonso. 2006. Detergent-resistant, ceramide-enriched domains in sphingomyelin/ceramide bilayers. *Biophys. J.* **90:** 903–914.
80. Deacon, E. M., T. R. Pettitt, P. Webb, T. Cross, H. Chahal, M. J. O. Wakelam, and J. M. Lord. 2002. Generation of diacylglycerol molecular species through the cell cycle: a role for 1-stearoyl, 2-arachidonyl glycerol in the activation of nuclear protein kinase C-βII at G2/M. *J. Cell Sci.* **115:** 983–989.
81. Floriddia, E. M., D. Pace, A. A. Genazzani, P. L. Canonico, F. Condorelli, and R. A. Billington. 2005. Sphingosine releases Ca^{2+} from intracellular stores via the ryanodine receptor in sea urchin egg homogenates. *Biochem. Biophys. Res. Commun.* **338:** 1316–1321.
82. Shaden, S., P. S. James, E. A. Howes, and R. Jones. 2004. Cholesterol efflux alters lipid raft stability and distribution during capacitation of boar spermatozoa. *Biol. Reprod.* **71:** 253–265.
83. Kobrinsky, E., A. I. Spielman, S. Rosenzweig, and A. R. Marks. 1999. Ceramide triggers intracellular calcium release via the IP(3) receptor in *Xenopus laevis* oocytes. *Am. J. Physiol.* **277:** C665–C672.
84. Runft, L. L., J. Watras, and L. A. Jaffe. 1999. Calcium release at fertilization of *Xenopus* eggs requires type I IP(3) receptors, but not SH2 domain-mediated activation of PLCγ or G(q)-mediated activation of PLCβ. *Dev. Biol.* **214:** 399–411.
85. Byrne, R. D., M. Gamier-Lhomme, K. Han, M. Dowicki, N. Michael, N. Totty, V. Zhendre, A. Cho, T. R. Pettit, M. J. Wakelam, et al. 2007. PLC-γ is enriched on poly-nuclear envelope assembly. *Cell. Signal.* **19:** 913–922.
86. Goldberg, E. M., and R. Zidovetzki. 1997. Effects of dipalmitoylglycerol and fatty acids on membrane structure and protein kinase C activity. *Biophys. J.* **73:** 2603–2614.
87. Mandani, S., A. Hichami, A. Legrand, J. Bellville, and N. A. Khan. 2001. Implication of acyl chain of diacylglycerols in activation of different isoforms of protein kinase C. *FASEB J.* **15:** 2595–2601.
88. Reynolds, N. J., H. S. Talwar, J. J. Baldassare, P. A. Henderson, J. T. Elder, J. J. Voorhees, and G. J. Fisher. 1993. Differential induction of phosphatidylcholine hydrolysis, diacylglycerol formation and protein kinase C activation by epidermal growth factor-α in normal human skin fibroblasts and keratinocytes. *Biochem. J.* **294:** 535–544.